Molecular Therapy
Nucleic Acids
Original Article

Targeting Repeated Regions Unique to a Gene Is an Effective Strategy for Discovering Potent and Efficacious Antisense Oligonucleotides

Lykke Pedersen,[1] Peter Hagedorn,[1] Jonas Vikeså,[1] Signe Tang Karlsen,[2] Pia Særmark,[2] Troels Koch,[1] and Morten Lindow[1]

[1]Therapeutic Modalities, Roche Pharma Research and Early Development, Roche Innovation Center Copenhagen, 2970 Hørsholm, Denmark; [2]The Bioinformatics Centre, Department of Biology, University of Copenhagen, 2100 Copenhagen, Denmark

Well-validated strategies for discovering potent and efficacious antisense oligonucleotides are central to realize the full therapeutic potential of RNA therapy. In this study, we focus on RNA targets where the same sequence of 16–20 nt is found in several regions across the RNA, and not in any other RNA. Targeting such unique repeated regions with oligonucleotides designed as gapmers and capable of recruiting RNase H has previously been proposed as a strategy for identifying potent gapmers. By sequence analysis of the human and monkey transcriptomes, we find that such unique repeated regions in RNA are often conserved between humans and monkeys, which allow pharmacodynamic effects to be evaluated in non-human primates before testing in humans. For eight potential RNA targets chosen in an unbiased fashion, we targeted their unique repeated regions with locked nucleic acid (LNA)-modified gapmers, and for six of them we identified gapmers that were significantly more potent and efficacious *in vitro* than non-repeat-targeting gapmer controls. We suggest a stochastic model for repeat-targeting gapmers that explains all effects observed so far and can help guide future work. Our results support the targeting of repeated regions as an effective strategy for discovering gapmer antisense oligonucleotides suitable for therapeutic development.

INTRODUCTION

The therapeutic potential of targeting RNA by antisense oligonucleotides (AONs) has been investigated intensely and the field has steadily progressed over the past four decades.[1] To date, five AONs have been approved for treatment, and there are currently at least 33 AONs in active clinical development around the world.[2,3] AONs can be designed as gapmers to allow the endogenous RNase H1 enzyme to bind to the duplex between gapmer and cRNA and cleave the RNA.[4,5] The mechanism by which RNase H1 cleaves RNA in DNA-RNA duplexes is well understood, and because the cleaved RNA fragments are rapidly degraded by endogenous nucleases, this has proven to be a robust therapeutic approach to reduce the levels of any RNA target of interest in both cytoplasm and nucleus.[6,7]

Any sequence region on a targeted RNA can in principle be engaged by gapmers, and both intronic and exonic regions can be targeted with comparable activities.[8] However, other region-specific factors, such as the presence of RNA self-structures,[9] RNase H sequence preferences,[10] and translational activity in the coding regions,[11] have been reported to influence the potency of gapmers. For libraries of gapmers tiled across a target RNA of interest, such factors help explain why gapmers targeting some regions can be substantially more potent than gapmers targeting outside these regions.[12] More recently, it has been demonstrated that potency can also be increased by targeting sequence regions that are repeated across an RNA of interest.[13] Specifically, for each of five RNA targets harboring 16- to 20-nt regions repeated between 2 and 35 times, the *in vitro* potency of gapmers targeting the repeats was found to be 2- to 8-fold higher compared to gapmers designed to target outside these regions.[13] To increase the chance that the gapmers targeting such repeated regions are sequence-specific with no or few unintended RNA off-targets, the identified repeated regions were also required to be unique to each RNA target and not found anywhere else in the transcriptome.[13] Interestingly, the sequence analysis performed by Vickers et al.[13] showed that close to 40% of all human pre-mRNAs harbors 16-nt regions repeated at least twice, while still being unique to that pre-mRNA,[13] suggesting that this strategy of targeting unique repeated regions could potentially find widespread use.

The present investigation was undertaken to validate this design strategy, as well as to further clarify how to best apply it AON drug development. First, we carried out sequence analysis to explore the extent to which human pre-mRNAs harbor unique repeated regions that are conserved also in monkeys. In AON drug development, gapmers are usually required to bind with perfect complementarity both to the human RNA target as well as to the ortholog RNA in a non-human primate species such as cynomolgus monkeys. This allows pharmacodynamics and pharmacological effects to be established in non-human

Received 4 July 2019; accepted 31 October 2019;
https://doi.org/10.1016/j.omtn.2019.10.040.

Correspondence: Lykke Pedersen, Therapeutic Modalities, Roche Pharma Research and Early Development, Roche Innovation Center Copenhagen, 2970 Hørsholm, Denmark.
E-mail: lykke.pedersen@roche.com

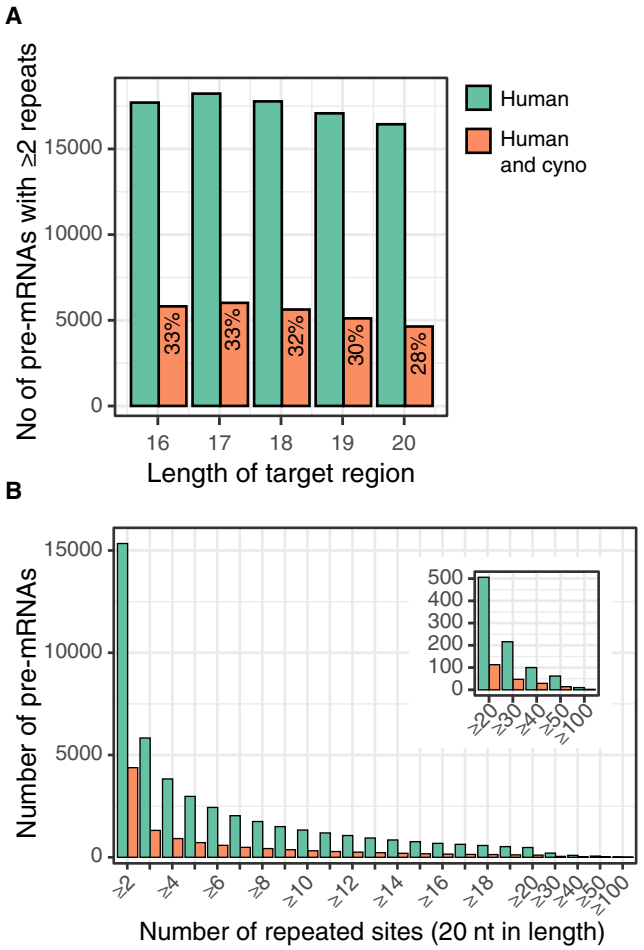

Figure 1. Sequence Analysis of Repeated Regions in the Human and Monkey Transcriptome

(A) The number of pre-mRNAs harboring two or more repeated regions as a function of the length of the target region (between 16 and 20 nt). Green bars show all human pre-mRNAs, and orange bars show pre-mRNAs where repeated regions are conserved between humans and cynomolgus monkeys. (B) For repeated regions that are at least 20 nt in length, the number of pre-mRNAs is shown as a function of the number of repeated regions. In the insert is shown the number of pre-mRNAs for 20–100 repeated regions.

primates before testing in humans.[14–16] We found that such unique and conserved repeated regions are present in one out of every eight pre-mRNAs. Second, in an unbiased fashion we selected eight different pre-mRNA targets harboring unique repeated regions and designed both repeat- and single region-targeting locked nucleic acid (LNA)-modified gapmers to evaluate activity *in vitro*. We found that for six out of the eight RNA targets, gapmers targeting repeated regions had significantly higher potency and maximal knockdown efficacy compared to gapmers targeting single, non-repeated regions. Specifically, we observed a 2- to 6-fold gain in potency, and up to 60% increase in knockdown efficacy. Third, we expanded on a previously reported kinetic model of gapmers[17] to also allow binding of gapmers to more than one distinct site per target. The expanded model correctly reproduced the improved potency and efficacy seen when the number of target sites per target is increased. The expanded model also predicted a saturation effect for very high numbers of repeated regions, as well as a differential sensitivity to changes in RNase H levels between repeated and non-repeated regions. Both of these predictions have also been observed experimentally,[13] supporting that the proposed model captures and explains the cellular mechanism of action of gapmers well.

Overall, our results confirm and clarify that if unique and conserved repeated regions can be identified in an RNA target of interest, which they can in one out of every eight human pre-mRNAs, targeting such regions can, in six out of the eight chosen RNA targets, i.e., three out of every four cases, be expected to be an effective design strategy for identifying potent and efficacious gapmers.

RESULTS

Identification of Unique Repeated Regions Conserved between Human and Cynomolgus Monkeys

The sequences of 50,916 human pre-mRNAs and 28,586 cynomolgus monkey pre-mRNAs annotated in the Ensembl database[18] (version GRCh38.p7) were analyzed for unique repeated regions of 16–20 nt in length (Table S1). Small RNA sequences shorter than 200 nt were not included in this analysis. The number of pre-mRNAs with two or more unique repeated regions is shown in Figure 1A, stratified into those found in humans and those conserved between humans and cynomolgus monkeys. As seen, around 17,500 human pre-mRNAs harbor repeated regions of 16 nt in length, and around 16,500 are found when requiring regions of at least 20 nt in length. When additionally requiring the repeated regions to be conserved between humans and monkeys, the number is reduced by around 70% at all lengths (Figure 1A). This reduction is explained both by the requirement of the repeated region to be conserved, and also due to only 40% of the human sequences having an ortholog identified in monkeys.[18] In Figure 1B the number of pre-mRNAs harboring 20-nt repeated regions is shown as a function of the number of repeats. As seen, higher numbers of repeats become increasingly rare, and more than 100 repeats are only seen in 17 human pre-mRNAs (insert in Figure 1B). Regions conserved between humans and monkeys consistently constitute around one third of the pre-mRNAs, irrespective of the number of repeats (Figure 1B). Overall, out of all 50,916 human sequences analyzed here, 13%, or approximately 1 out of every 8, harbors conserved repeated regions (Table S1).

Experimental Validation of Repeat Targeting Strategy

Among the 3,569 pre-mRNAs harboring five- or more unique repeated regions, eight RNA targets were randomly chosen (Table 1), subject to the following two criteria: (1) since we intended to evaluate knockdown of each of these targets in HeLa cells, only targets that were expected to be expressed in this cell line were chosen;[19] and (2) also, to ensure that we would be working with relatively well-established RNA targets that had already been investigated previously to some extent, only those mentioned in at least 30 scientific papers indexed in PubMed were chosen.[20] We designed 96 LNA-modified

Table 1. Pre-mRNA Targets Harboring Repeated Regions Used for Evaluation

Symbol	Name	Repeats
CSNK1D	casein kinase 1 delta	10–11 and 23–27
ERC1	ELKS/RAB6-interacting/CAST family member 1	19–20
FNDC3B	fibronectin type III domain containing 3B	7
GSK3B	glycogen synthase kinase 3 beta	5 and 5
PIAS4	protein inhibitor of activated STAT4	5–6
RB1	RB transcriptional corepressor 1	24–25
TOM1	target of myb1 membrane trafficking protein	7 and 7–9
UBE3C	ubiquitin protein ligase E3C	6 and 6

The number of repeats is shown as a range, e.g., 23–27, if gapmers of different lengths target slightly different number of repeats. Often, shorter gapmers can target more repeats. When two different repeated regions are targeted, the number of each is separated by "and," e.g., 5 and 5.

gapmers with full phosphorothioate backbones against these eight targets. For four of the targets, *ERC1*, *FNDC3B*, *PIAS1*, and *RB1*, eight gapmers were designed against each, four to the repeated region and four to a non-repeated region. For the remaining four targets, *CSNK1D*, *GSK3B*, *TOM1*, and *UBE3C*, two different repeated regions were identified in each of them, and therefore 16 gapmers were designed against each target, four to each of the two different repeated regions, respectively, and, similarly, four to each of two different non-repeated regions (Table S2; Figure S1). The non-repeated regions for each target were selected at random among all possible non-repeated target regions, identified following a computational workflow as described previously,[21] and, just as for the repeated regions, required to be unique and only found in that target. To control for possible length-dependent biases, the gapmers designed against each target and each region covered lengths of 14, 16, 18, and 20 nt, and the number of LNA modifications were adjusted to be between one and four in each flank, so that all 96 gapmers were predicted by a nearest neighbor model[17] to have similar binding affinities to their RNA target region.

Knockdown of each of the eight RNA targets by the LNA gapmers was evaluated by qRT-PCR in HeLa cells (n = 3) at eight different concentrations ranging from 0.01 to 32.1 μmol/L. Sigmoidal concentration-response curves (CRCs) were fitted to the resulting data (Figure 2A; Table S3), and potency and efficacy were estimated from this (Table S2). Potency is here defined as the inverse of the half-maximal effect concentration, EC_{50}, and efficacy as the maximally obtainable knockdown. The observed CRCs vary widely both with respect to potency and efficacy (Figure 2A). Gapmers that reduced mRNA target levels by less than 15%, even at the highest concentration tested, were judged as inactive and excluded from further analysis (two times the SD observed between PBS controls, indicated as dashed lines in Figure 2A), As seen in Figure 2A, for most of the targets, repeat matching gapmers (blue lines) are more potent and/or efficacious than single matching gapmers (red lines). This observation is quantified in Figures 2B–2E.

Figure 2B shows the most potent single and repeat matching gapmers across all eight targets. For five out of the eight targets, *CSNK1D*, *FNDC3B*, *GSK3B*, *PIAS4*, and *RB1*, a repeat matching gapmer was found to be significantly more potent than the most potent single matching gapmer designed against that target. For those same five targets as well as for *ERC1*, the maximal knockdown efficacy increased significantly as well (Figure 2C). For *TOM1*, two of the single matching gapmers were clearly the most potent and efficacious gapmers identified (Figures 2A–2C), and for *UBE3C* there was no clear difference between single and repeat matching gapmers (Figures 2A–2C). In summary, significant improvements in potency and/or efficacy were seen for six out of eight targets, with as high as a 6-fold improved potency for *CSNK1D* (Figure 2B) and a 60% increase in efficacy observed for *PIAS4* (Figure 2C). Overall, across all eight targets, the strategy of targeting repeated regions generally resulted in gapmers that were significantly more potent (Figure 2D) and efficacious (Figure 2E), compared to single matching gapmers. On average, around 2-fold improved potency and a 30% increase in efficacy can be expected (Figures 2D and 2E, respectively).

Stochastic Modeling of Gapmers Binding to Repeated Regions Explains Their Mechanism of Action

The system of reactions for gapmer binding to RNA in non-repeated or repeated regions, and subsequent cleavage by RNase H, is shown as a schematic in Figure 3A. Here, gapmer, denoted by O, can bind to the target RNA, T, at either of *n* different target sites in a reversible manner, to form the duplex, OT (Figure 3). This duplex between gapmer and RNA is the substrate for the RNase H enzyme, E, which, when bound to the duplex forms the complex OTE. Once the RNA is cleaved by the enzyme, changing from T to C in the OCE complex, enzyme and gapmers dissociate from it, and the cleaved, exposed, and unprotected ends of the RNA will be rapidly (instantly in the model) degraded by exonucleases. The RNA target is produced at a constant rate and, besides the gapmer-mediated degradation, also naturally degraded following first-order kinetics (Figure 3A).

The time evolution of the system of reactions described above was simulated stochastically using the Gillespie[22] algorithm. An example of running such a simulation over time is shown in Figure 4A for target RNA with just a single target region (orange lines) as well as for target RNA harboring a region repeated 10 times (red lines). The system initially consists only of free RNA, gapmer, and RNase H, but as time progresses, they start to associate, dissociate, and react with each other, until equilibrium is reached at around 120 min (Figure 4A). All reaction rates and other model parameters are the same as used previously,[17] and they are included as Table S4 for completeness. The only extra parameter introduced in the expanded model is the number of repeated target sites per RNA target. However, this expansion introduces a dependency between repeated regions on the same target, which can only be solved by stochastic simulation, and not by numerical integration of ordinary differential equations as done previously.[17]

To explore the behavior of the model, first, the system of reactions was simulated for non-repeated RNA targets as well as for RNA

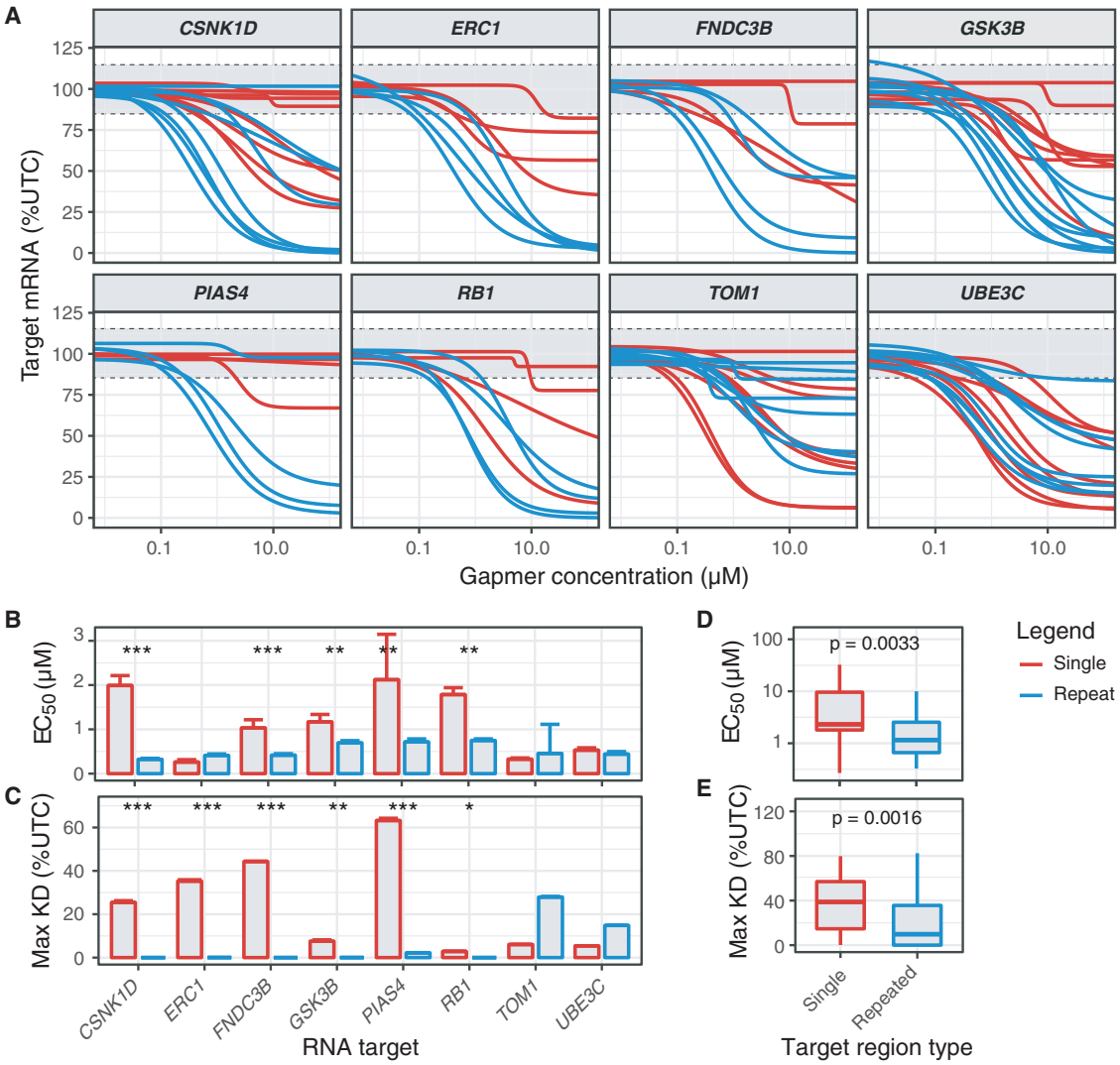

Figure 2. Experimental Evaluation of RNA Target Knockdown in HeLa Cells

(A) For each gapmer a sigmoidal concentration-response curve was fitted to the measured mRNA levels. Red lines indicate gapmers targeting repeated regions. Blue lines indicate gapmer targeting non-repeated, single regions. Dashed lines and gray box indicate ± 2 SD of mRNA levels of PBS controls. All data points can be found in Table S3. (B and C) Barplots for average and SD of EC_{50} (B) and maximal knockdown efficacy (C) as estimated from the fitted CRCs. For each target, the most potent and efficacious gapmers targeting repeated (red bars) and non-repeated regions (blue bar) were chosen, and the significance of the differences between them was evaluated using a *Z* test for EC_{50} estimates and a t test for efficacy estimates. *$p < 0.05$, **$p < 0.01$, ***$p < 0.001$. (D and E) Boxplots for all EC_{50} (D) and efficacy estimates (E) across all eight targets, stratified by whether gapmers targeted repeated (red boxes) or non-repeated, single (blue boxes) regions. The significance of the difference between distributions is calculated by a one-sided Kolmogorov-Smirnov test.

targets with an increasing number of repeated regions. When varying the number of gapmers, total RNA at steady state relative to initial RNA levels reproduces sigmoidal concentration-response behavior as expected (Figure 4B). With an increasing number of repeated regions, both potency (Figures 4B and 4C) and maximal knockdown efficacy (Figures 4B and 4D) is improved. The incremental improvement is largest for low numbers of repeats, however, suggesting a saturation effect at high numbers of repeated regions where additional regions have negligible added benefit (Figures 4C and 4D).

Second, the effect of changing the number of RNase H enzymes was explored (Figure 4E). For both RNA harboring only non-repeated target regions (orange lines), as well as for RNA harboring target regions repeated 10 times (red lines), higher RNase H enzyme levels improved potency and efficacy (compare dashed and solid lines in Figure 4E). As also shown in Figure 4E, the increased levels of RNase H have a greater effect on potency when gapmers target non-repeated regions (orange lines, dashed versus solid) than when gapmers target repeated regions (red lines, dashed versus solid). When calculating fold changes in potency between gapmers targeting single and

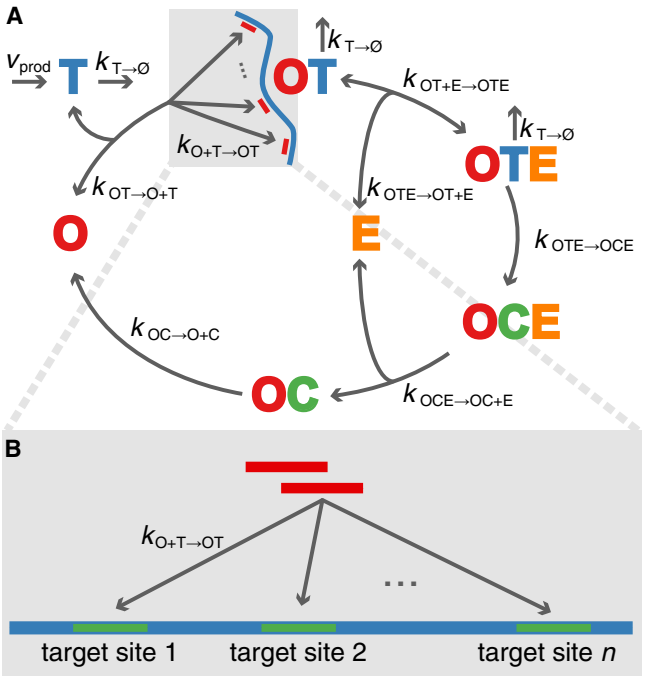

Figure 3. Schematic of the Modeled Reactions

(A) Initially, the oligonucleotide gapmer (O) binds to the RNA target (T) and forms the OT complex, which recruits the enzyme (E). Within the OTE complex, the target is cleaved (C) to form OCE. The enzyme and then the gapmer dissociate from the cleaved target to enter a new round of catalysis. The target has a constant production rate denoted by ν_{prod}, and a basal gapmer- and RNase H-independent degradation rate, $k_{T\rightarrow\varnothing}$. Here, ∅ denotes completely degraded target. The dissociation rate of enzyme from OT and OC is assumed to be the same. (B) For gapmers binding repeated regions on the RNA target, each of the *n* target sites on a given RNA can be engaged independently of each other and elicit cleavage and degradation.

repeated regions, respectively, this differential effect on potency saturates as the RNase H levels become very high (Figure 4F). A contributing factor to explaining the relatively large differences in maximal knockdown efficacy of 20%–60% between repeated and non-repeated regions observed in particular for *CSKN1D*, *ERC1*, *FNDC3B*, and *PIAS4* (Figure 2C) could therefore be a relatively low level of RNase H enzyme in these cells.

We and others have suggested that an optimal binding affinity for gapmers exists that allows maximal potency to be achieved.[17,23] This stems from the observation that the same gapmer is expected to be involved in multiple rounds of binding, cleavage, and release from target RNA in cells. The stochastic model also predicts the existence of such an optimal binding affinity, and it suggests that as the number of repeats increases, the optimal binding affinity becomes lower (Figure S1). That is, slightly weaker binding gapmers are needed to achieve optimal potency against repeated regions compared to non-repeated regions. The reason for this is that as the effective number of target regions is increased, the propensity to dissociate from one target RNA, in order to be able to associate with another target RNA, becomes increasingly important.

DISCUSSION

In this study, we validated the previously proposed strategy of targeting unique repeated regions in RNA for discovering potent and efficacious gapmers. In an unbiased manner, only for the purpose of evaluating the strategy, we selected eight RNA targets harboring unique repeated regions. Using standard design criteria, we targeted gapmers to the repeated regions as well as outside those regions and evaluated potency and maximal target knockdown efficacy in HeLa cells by qRT-PCR. We found significantly increased potency and/or efficacy for gapmers targeted to unique repeated regions for six of the eight RNA targets, suggesting that this can be expected to be a successful strategy three out of four times. Moreover, we also showed that about one third of the unique repeated regions are conserved between humans and cynomolgus monkeys. Most gapmer drug discovery programs require such conservation to allow pharmacodynamic effects to be evaluated in non-human primates. That unique repeated regions are relatively often conserved makes the strategy of targeting them much more useful in practice. Finally, the increases in potency and efficacy are well explained by our kinetic model, and they follow straightforwardly from the increased effective concentration of target sites. Our model also predicts more complex behaviors, such as the saturation effect at a high number of repeated regions, the differential effects on potency and efficacy as a function of the intracellular levels of RNase H, and decreased optimal binding affinity as the number of repeated regions increases. That the target engagement mechanism by which gapmers affect RNA is well captured by kinetic modeling, as shown here, could support future drug discovery projects by enabling more precise pharmacokinetic and pharmacodynamic modeling in non-human primates for dose projections to humans.

Among the eight RNA targets evaluated experimentally here, the number of repeated regions is not simply related to the effect size on potency and maximal knockdown efficacy. This has also been observed previously.[13] Some repeated regions might be inaccessible due to RNA structures or protein binding. The number of repeated regions that are actually available for engagement by gapmers could therefore be smaller than the number of regions present in the sequence. This may partly explain the lack of correlation between number of repeats and magnitude of the gain in potency and efficacy. Many other factors, such as productive cellular uptake,[24] subcellular distribution,[25] and sequence preferences of the RNase H enzyme,[10] have also been reported to affect potency and efficacy in a sequence-specific manner, and, similarly, may therefore contribute to the lack of correlation. Incidentally, such considerations can also explain why repeated regions in *TOM1* and *UBE3C* are less potent or effective than non-repeated regions. Either the non-repeated regions chosen for those two targets are simply highly suited for targeting due to sequence-specific factors such as those mentioned above, or oppositely the repeated regions are very unsuited. Another reason for the lack of correlation, as suggested by the modeling results, could be that the biggest impact on potency and efficacy is seen when going from single regions to regions repeated just a few times. The relative improvement in potency and efficacy gets smaller and smaller as the

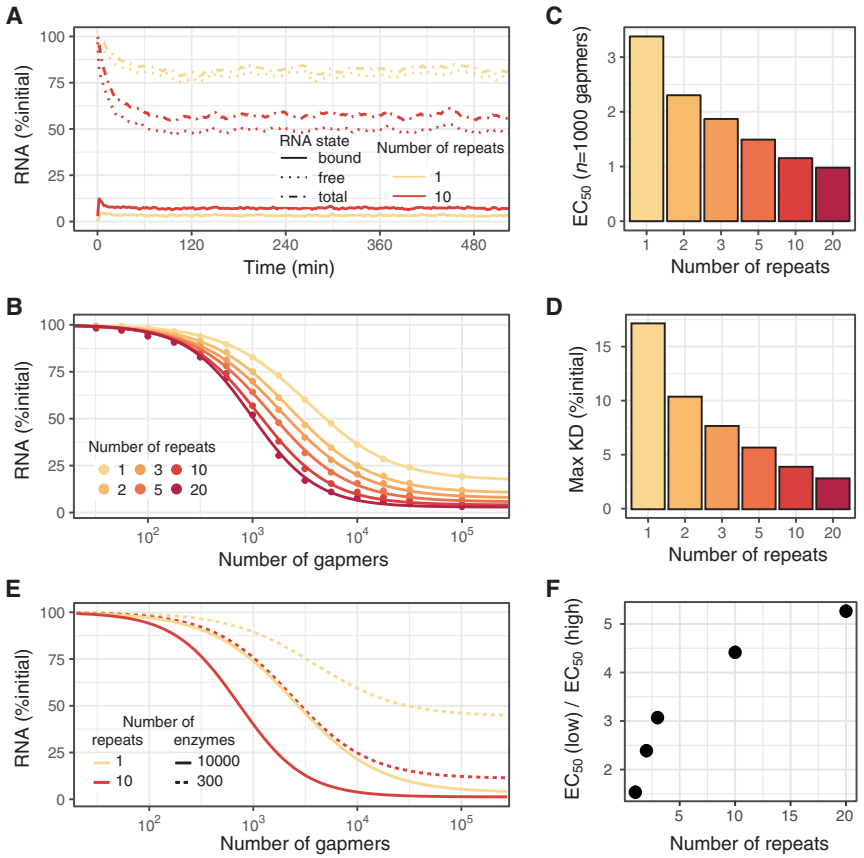

Figure 4. Model Simulations and Predictions

(A) Time-resolved simulation of the relative concentrations of free, bound and total RNA for 1 or 10 repeated target sites on the RNA. (B) Simulated concentration-response curves (CRCs) for 1, 2, 3, 5, 10, and 20 target sites per RNA target. (C and D) From the CRCs, (C) half-maximal concentration, EC_{50}, and (D) maximal knockdown efficacy are estimated. The greatest change in potency and efficacy occurs when increasing the number of repeated target sites from one to two. (E) Simulated CRCs for 10,000 and 300 RNase H enzymes (dotted versus solid lines, respectively) and for 1 and 10 repeated target sites (yellow versus red lines, respectively). (F) Ratio of estimated EC_{50}s for 10,000 (high) and 300 (low) RNase H enzymes as a function of the number of repeated regions in the target RNA.

number of repeats increase. For the eight targets evaluated here, harboring regions repeated at least five times, which could mean that most of the benefit of repeated regions has already been realized.

To allow for a fair comparison of the effectiveness of each strategy, the gapmers for this study were designed in equal numbers and using the same criteria irrespective of whether they targeted repeated or non-repeated regions. Specifically, they are all targeting unique 20-nt regions found only in the intended target, covering lengths from 14 to 20 nt to allow for individual differences in accessibility and RNase H sequence preferences between target regions, and with LNA load in the flanks adjusted to reach a predicted change in free energy of binding close to −22 kcal/mol irrespective of length. A binding affinity in this range has previously been identified as optimal for LNA gapmers targeting non-repeated regions.[17] It could be that since the optimal binding affinity for gapmers targeting repeated regions is predicted to be a bit weaker than for gapmers targeting non-repeated regions, as discussed above, even larger differences in effectiveness between repeated and non-repeated regions might have been achieved if the predicted binding affinity had been fixed at lower common value.

The biological functions of the eight RNA targets selected for this study are all being actively investigated, and the potent and efficacious gapmers identified here might provide good starting points for future functional studies exploring therapeutic potential. For example, knockdown of *RB1* has been shown to enhance adult nerve regeneration,[26] both *UBE3C* and *GSK3B* have been associated with development and progression of hepatocellular carcinoma (HCC),[27,28] and *ERC1* has been shown to be required for efficient replication of dengue virus.[29]

In our laboratories, for those discovery projects where we pursue RNA target cleavage by RNase H, we typically commit to synthesize and screen hundreds to thousands of gapmers. Because of the results reported here as well as those previously reported,[13] our standard practice is to analyze the pre-mRNA target sequence for repeated regions as well as multiple other features that could potentially impact activity or tolerance.[21] When unique and conserved repeated regions are identified, we make sure to design gapmers targeting these regions in addition to the comprehensive targeting of non-repeated regions.

At the heart of the steady progression of AONs toward the clinic lies the commitment in the research field to design and carry out well-controlled and adequately powered experiments,[30] as well as the willingness to commit the resources needed for careful independent validation of key observations. Such activities are key to establishing solid and reliable stepping stones for future developments in the field. With this study, where we successfully validated and clarified the development potential of the strategy of targeting unique repeated regions with gapmers, we hope to have provided one more stepping stone, and progressed the field yet another small step closer toward realizing its full therapeutic potential.

MATERIALS AND METHODS

Identification of Transcripts with Uniquely Repeated Regions and Design of Gapmers

The pre-mRNA sequences transcribed from 58,336 human genes were retrieved from the Ensembl database release 96.[18] Among these,

a set of 3,569 sequences were identified by sequence analysis containing five or more repeated regions of at least 20 nt in length that were not present in any other sequence. Eight RNA targets were selected from this set of 3,569 pre-mRNAs with uniquely repeated regions by the following procedure: first, a pre-mRNA was chosen randomly from among the 3,569; second, the expression of this pre-mRNA in HeLa cells was evaluated by visual inspection of read coverage using CLC Genomics Workbench (QIAGEN) based on publicly available RNA sequencing (RNA-seq) data from HeLa cells;[19] and third, if coverage was judged sufficient to be measurable also by qRT-PCR, the pre-mRNA gene symbol was queried using the PubMed search engine, which accesses the MEDLINE bibliographic database covering medical literature.[20] If more than 30 citations were returned, the pre-mRNA was selected, otherwise it was discarded. This procedure was repeated until eight RNA targets had been selected in this manner. For each of the eight selected RNA targets, gapmers of length 14, 16, 18, and 20 nt were designed to target the repeated region (Table S4). The number of LNAs in the flanks of each gapmer was adjusted to reach a predicted change in free energy of binding of around −22 ± 2 kcal/mol (mean ± SD). This is in the range where the optimal binding affinity with respect to LNA-gapmer potency has previously been identified to be for a number of RNA targets.[17] Similarly, control gapmers of length 14, 16, 18, and 20 nt were designed for each of the eight chosen RNA targets to bind to regions not repeated. For each target, these non-repeated regions were randomly selected among all possible non-repeated regions, identified as previously described.[21] Specifically, to be electable, the 20-nt non-repeated regions were required to be unique for that target, that is, the same region must not be present in any other RNA. As for the gapmers targeting repeated regions, the gapmers targeting non-repeated regions were designed to reach predicted changes in free energy of binding of around −22 ± 2 kcal/mol.

Oligonucleotide Synthesis and Purification

LNA-modified AONs were synthesized with complete phosphorothioate backbones using standard phosphoramidite protocols on an Expedite 8900 synthesizer with a Multiple Oligonucleotide Synthesis System unit (ABI, Foster City, CA, USA). The oligonucleotides were purified by reverse-phase high-performance liquid chromatography. The oligonucleotides were dissolved in PBS and the oligonucleotide concentration in solution determined using Beer-Lambert's law by calculating the extinction coefficient and measuring UV absorbance. Oligonucleotide identity and purity were determined by reversed-phase ultra-performance liquid chromatography coupled to mass spectrometry (UPLC-MS).

RNA Analysis by qRT-PCR in HeLa Cells

The HeLa cell line was purchased from the European Collection of Authenticated Cell Cultures (through Sigma-Aldrich, Denmark) and maintained as recommended by the supplier in a humidified incubator at 37°C with 5% CO_2. Cells were seeded with a density of 2,500 HeLa cells/well in a 96 multi-well plate with culture media and incubated for 24 h before addition of oligonucleotides dissolved in PBS at final concentrations of 0.01, 0.031, 0.1, 0.31, 1, 3.21, 10, and 32.1 μmol/L, respectively. Cells were harvested 3 days later and RNA was extracted using the PureLink Pro 96 total RNA purification kit according to the manufacturer's instructions (Thermo Fisher Scientific). Transcripts levels were quantified using qScript XLT 1-Step RT-qPCR ToughMix (Quantabio) according to the manufacturer's instructions. The following TaqMan assays were used: CSNK1D (Hs00371197_m1), ERC1 (Hs01553904_m1), FND3C (Hs00981550_m1), GSK3B (Hs01047718_m1), PIAS4 (Hs01071948_m1), RB1 (Hs01078066_m1), TOM1 (Hs00193953_m1), UBE3C (Hs00904539_m1), and glyceraldehyde-3-phosphate dehydrogenase (GAPDH; 4326317E). The ViiA 7 real-time PCR system was used for amplification and detection. Transcript levels were normalized to GAPDH and presented as percentage change relative to average levels in mock-treated controls. All qRT-PCR data are available in Table S3.

Stochastic Simulation of the Kinetic Model

The Gillespie stochastic simulation algorithm (SSA) is a stochastic model that deals with simulations of population changes in discrete time for finite populations. For modeling the reactions between AON, RNA target, and RNase H enzyme, we are using an R implementation of the Gillespie SSA[31]. Model parameters are listed in Table S4.

SUPPLEMENTAL INFORMATION

Supplemental Information can be found online at https://doi.org/10.1016/j.omtn.2019.10.040.

AUTHOR CONTRIBUTIONS

J.V. designed the laboratory experiments. L.P., P.S., and S.T.K. developed the model. L.P., P.H.H., M.L. and T.K. wrote the paper. All authors have approved the final manuscript.

CONFLICTS OF INTEREST

S.T.K., P.S., M.L., and T.K. declare no competing interests. L.P., P.H., and J.V. are employees of F. Hoffmann-La Roche, a company developing RNA-targeted therapeutics.

ACKNOWLEDGMENTS

The authors would like to thank Kirsten Nymann Petersen for the synthesis of the AONs.

REFERENCES

1. Watts, J.K., and Corey, D.R. (2012). Silencing disease genes in the laboratory and the clinic. J. Pathol. *226*, 365–379.
2. Crooke, S.T., Witztum, J.L., Bennett, C.F., and Baker, B.F. (2018). RNA-targeted therapeutics. Cell Metab. *27*, 714–739.
3. Keam, S.J. (2018). Inotersen: first global approval. Drugs *78*, 1371–1376.
4. Walder, R.Y., and Walder, J.A. (1988). Role of RNase H in hybrid-arrested translation by antisense oligonucleotides. Proc. Natl. Acad. Sci. USA *85*, 5011–5015.
5. Wu, H., Lima, W.F., Zhang, H., Fan, A., Sun, H., and Crooke, S.T. (2004). Determination of the role of the human RNase H1 in the pharmacology of DNA-like antisense drugs. J. Biol. Chem. *279*, 17181–17189.
6. Castanotto, D., Lin, M., Kowolik, C., Wang, L., Ren, X.-Q., Soifer, H.S., Koch, T., Hansen, B.R., Oerum, H., Armstrong, B., et al. (2015). A cytoplasmic pathway for gapmer antisense oligonucleotide-mediated gene silencing in mammalian cells. Nucleic Acids Res. *43*, 9350–9361.

7. Liang, X.-H., Sun, H., Nichols, J.G., and Crooke, S.T. (2017). RNase H1-dependent antisense oligonucleotides are robustly active in directing RNA cleavage in both the cytoplasm and the nucleus. Mol. Ther. *25*, 2075–2092.

8. Kamola, P.J., Kitson, J.D., Turner, G., Maratou, K., Eriksson, S., Panjwani, A., Warnock, L.C., Douillard Guilloux, G.A., Moores, K., Koppe, E.L., et al. (2015). In silico and in vitro evaluation of exonic and intronic off-target effects form a critical element of therapeutic ASO gapmer optimization. Nucleic Acids Res. *43*, 8638–8650.

9. Vickers, T.A., Wyatt, J.R., and Freier, S.M. (2000). Effects of RNA secondary structure on cellular antisense activity. Nucleic Acids Res. *28*, 1340–1347.

10. Kielpinski, L.J., Hagedorn, P.H., Lindow, M., and Vinther, J. (2017). RNase H sequence preferences influence antisense oligonucleotide efficiency. Nucleic Acids Res. *45*, 12932–12944.

11. Liang, X.-H., Nichols, J.G., Sun, H., and Crooke, S.T. (2018). Translation can affect the antisense activity of RNase H1-dependent oligonucleotides targeting mRNAs. Nucleic Acids Res. *46*, 293–313.

12. Laxton, C., Brady, K., Moschos, S., Turnpenny, P., Rawal, J., Pryde, D.C., Sidders, B., Corbau, R., Pickford, C., and Murray, E.J. (2011). Selection, optimization, and pharmacokinetic properties of a novel, potent antiviral locked nucleic acid-based antisense oligomer targeting hepatitis C virus internal ribosome entry site. Antimicrob. Agents Chemother. *55*, 3105–3114.

13. Vickers, T.A., Freier, S.M., Bui, H.-H., Watt, A., and Crooke, S.T. (2014). Targeting of repeated sequences unique to a gene results in significant increases in antisense oligonucleotide potency. PLoS ONE *9*, e110615.

14. Elmén, J., Lindow, M., Schütz, S., Lawrence, M., Petri, A., Obad, S., Lindholm, M., Hedtjärn, M., Hansen, H.F., Berger, U., et al. (2008). LNA-mediated microRNA silencing in non-human primates. Nature *452*, 896–899.

15. Lindholm, M.W., Elmén, J., Fisker, N., Hansen, H.F., Persson, R., Møller, M.R., Rosenbohm, C., Ørum, H., Straarup, E.M., and Koch, T. (2012). PCSK9 LNA antisense oligonucleotides induce sustained reduction of LDL cholesterol in nonhuman primates. Mol. Ther. *20*, 376–381.

16. Kornbrust, D., Cavagnaro, J., Levin, A., Foy, J., Pavco, P., Gamba-Vitalo, C., and Guimond, A. (2013). Oligo safety working group exaggerated pharmacology subcommittee consensus document. Nucleic Acid Ther. *23*, 21–28.

17. Pedersen, L., Hagedorn, P.H., Lindholm, M.W., and Lindow, M. (2014). A kinetic model explains why shorter and less affine enzyme-recruiting oligonucleotides can be more potent. Mol. Ther. Nucleic Acids *3*, e149.

18. Zerbino, D.R., Achuthan, P., Akanni, W., Amode, M.R., Barrell, D., Bhai, J., Billis, K., Cummins, C., Gall, A., Girón, C.G., et al. (2018). Ensembl 2018. Nucleic Acids Res. *46* (D1), D754–D761.

19. Klijn, C., Durinck, S., Stawiski, E.W., Haverty, P.M., Jiang, Z., Liu, H., Degenhardt, J., Mayba, O., Gnad, F., Liu, J., et al. (2015). A comprehensive transcriptional portrait of human cancer cell lines. Nat. Biotechnol. *33*, 306–312.

20. Sayers, E.W., Agarwala, R., Bolton, E.E., Brister, J.R., Canese, K., Clark, K., Connor, R., Fiorini, N., Funk, K., Hefferon, T., et al. (2019). Database resources of the National Center for Biotechnology Information. Nucleic Acids Res. *47* (D1), D23–D28.

21. Pedersen, L., Hagedorn, P.H., and Koch, T. (2019). Identifying suitable target regions and analyzing off-target effects of therapeutic oligonucleotides. Methods Mol. Biol. *2036*, 261–282.

22. Gillespie, D.T. (1977). Exact stochastic simulation of coupled chemical-reactions. J. Phys. Chem. *81*, 2340–2361.

23. Yamamoto, T., Fujii, N., Yasuhara, H., Wada, S., Wada, F., Shigesada, N., Harada-Shiba, M., and Obika, S. (2014). Evaluation of multiple-turnover capability of locked nucleic acid antisense oligonucleotides in cell-free RNase H-mediated antisense reaction and in mice. Nucleic Acid Ther. *24*, 283–290.

24. Hung, G., Xiao, X., Peralta, R., Bhattacharjee, G., Murray, S., Norris, D., Guo, S., and Monia, B.P. (2013). Characterization of target mRNA reduction through in situ RNA hybridization in multiple organ systems following systemic antisense treatment in animals. Nucleic Acid Ther. *23*, 369–378.

25. Liang, X.-H., Sun, H., Shen, W., and Crooke, S.T. (2015). Identification and characterization of intracellular proteins that bind oligonucleotides with phosphorothioate linkages. Nucleic Acids Res. *43*, 2927–2945.

26. Christie, K.J., Krishnan, A., Martinez, J.A., Purdy, K., Singh, B., Eaton, S., and Zochodne, D. (2014). Enhancing adult nerve regeneration through the knockdown of retinoblastoma protein. Nat. Commun. *5*, 3670.

27. Jiang, J.-H., Liu, Y.-F., Ke, A.-W., Gu, F.-M., Yu, Y., Dai, Z., Gao, Q., Shi, G.-M., Liao, B.-Y., Xie, Y.-H., et al. (2014). Clinical significance of the ubiquitin ligase UBE3C in hepatocellular carcinoma revealed by exome sequencing. Hepatology *59*, 2216–2227.

28. Zhang, N., Liu, X., Liu, L., Deng, Z., Zeng, Q., Pang, W., Liu, Y., Song, D., and Deng, H. (2018). Glycogen synthase kinase-3β inhibition promotes lysosome-dependent degradation of c-FLIP$_L$ in hepatocellular carcinoma. Cell Death Dis. *9*, 230.

29. Khadka, S., Vangeloff, A.D., Zhang, C., Siddavatam, P., Heaton, N.S., Wang, L., Sengupta, R., Sahasrabudhe, S., Randall, G., Gribskov, M., et al. (2011). A physical interaction network of dengue virus and human proteins. Mol. Cell. Proteomics *10*, M111.012187.

30. Gagnon, K.T., and Corey, D.R. (2019). Guidelines for experiments using antisense oligonucleotides and double-stranded RNAs. Nucleic Acid Ther. *29*, 116–122.

31. Pineda-Krch, M. (2008). GillespieSSA: implementing the stochastic simulation algorithm in R. J. Stat. Softw. *25*, 1–18.